Inorganic Chemistry

Article

pubs.acs.org/IC

A Bis(terpyridine)ruthenium Complex with Three Redox-Active Amine Sites: Electrochemical, Optical, and Computational Studies

You-Ming Zhang,[†,‡,§] Si-Hai Wu,[†,§] Chang-Jiang Yao,[†] Hai-Jing Nie,[†] and Yu-Wu Zhong*[,†,⊥]

[†]Beijing National Laboratory for Molecular Sciences, CAS Key Laboratory of Photochemistry, Institute of Chemistry, Chinese Academy of Sciences, Beijing 100190, People's Republic of China

[‡]College of Chemistry, Xiangtan University, Xiangtan 411105, People's Republic of China

[⊥]State Key Laboratory of Coordination Chemistry, Nanjing University, Nanjing 210093, People's Republic of China

Supporting Information

ABSTRACT: Two ruthenium complexes, $[Ru(NN)(ttpy)]^{2+}$ and $[Ru(NN)(daatpy)]^{2+}$, have been designed and prepared, where NN is bis(amine) ligand 4′-tolyl-5,5″-bis(di-*p*-anisylamino)-2,2′:6′,2″-terpyridine, ttpy is 4′-tolyl-2,2′:6′,2″-terpyridine, and daatpy is 4′-di-*p*-anisylamino-2,2′:6′,2″-terpyridine. Complex $[Ru(NN)(daatpy)]^{2+}$ contains three redox-active amine groups and has been characterized by single-crystal X-ray analysis. These two complexes display much-enhanced light absorption capabilities with respect to the prototype compound $[Ru(tpy)_2]^{2+}$ (tpy = 2,2′:6′,2″-terpyridine), which has been rationalized on the basis of time-dependent density functional theory calculations. Electrochemical and optical studies showed that there was little electronic coupling between two amine sites in complex $[Ru(NN)(ttpy)]^{2+}$. On the other hand, a ligand-to-ligand ($N \rightarrow N'^{\bullet+}$) charge-transfer band has been observed at 1430 nm for singly and doubly oxidized forms of $[Ru(NN)(daatpy)]^{2+}$, and an electronic coupling parameter of 1000 cm^{-1} was derived using the Hush formula. This band is interpreted as a charge transfer from the neutral amine of the daatpy ligand to oxidized aminium units in the NN ligand.

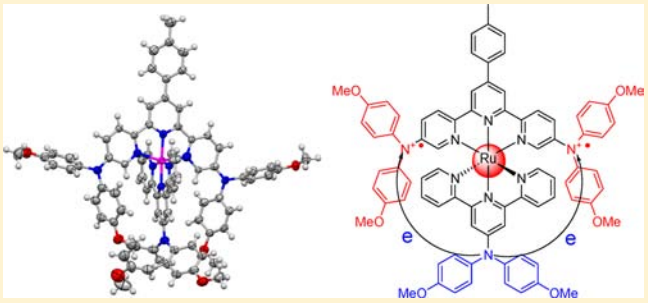

INTRODUCTION

Polypyridine transition-metal complexes have been the focus of intensive research activities because of their attractive electronic and optical properties.[1] Many of them feature chemically reversible metal-associated redox processes and broad metal-to-ligand charge-transfer (MLCT) transitions in the visible region. They have been used in a wide range of applications including organic light-emitting devices (OLEDs),[2] dye-sensitized solar cells,[3] mixed-valence chemistry,[4] and electrochromic devices.[5] On the other hand, triarylamines are one of the most popular organic optoelectronic materials,[6] well-known for their good electron-donating and hole-transporting abilities. They have been widely used in many optoelectronic devices, such as OLEDs[7] and photovoltaic devices.[8]

Hybrid compounds consisting of polypyridine transition-metal complexes and triarylamines are expected to yield materials with appealing optoelectronic properties.[9] For instance, the incorporation of triarylamine units into transition-metal dyes has been reported to greatly enhance light absorption and, hence, the photovoltaic efficiency of solar cells.[10] Ruthenium complexes containing peripheral diphenylamino groups have been used to prepare metallopolymeric films through oxidative electropolymerization.[11] Recently, Lemaire and co-workers documented the ferromagnetic coupling between a triarylaminium radical cation and a Mn^{2+} center supported by 2,2′-bipyridine.[12]

We are particularly interested in using polypyridine metal complexes as a backbone to mediate amine−amine electronic coupling. A large number of mixed-valence systems with triarylamines as charge-bearing sites have been reported to investigate the amine−amine electronic coupling.[13] However, most systems are bridged with a purely organic component except for a few examples.[14] We recently reported on a $[Ru(tpy)_2]$-bridged bis-amine compound $[Ru(daatpy)_2]^{2+}$ (Figure 1; tpy = 2,2′:6′,2″-terpyridine and daatpy = 4′-di-*p*-anisylamino-2,2′:6′,2″-terpyridine) and observed the presence of an intervalence charge-transfer (IVCT) band between two amine sites after monooxidation.[15] In another report, the lateral chelation of a metal component to 2,2′-bipyridine was found to enhance the electronic coupling between two amines on the 5 and 5′ positions of the ligand.[16] These results encouraged us to investigate the possible metal-mediated electronic communication between two amines on the 5 and 5″ positions of a tpy compound. A possible candidate for this purpose is represented as [M(5,5″-N,N-tpy)] in Figure 1, which will require the synthesis of 5,5″-dibromo-2,2′:6′,2″-terpyridine. We note that, although an improved procedure has been disclosed for the synthesis of this bromide,[17] four-step reactions are necessary from commercially available sources. Thus, we turned our

Received: May 15, 2012
Published: October 17, 2012

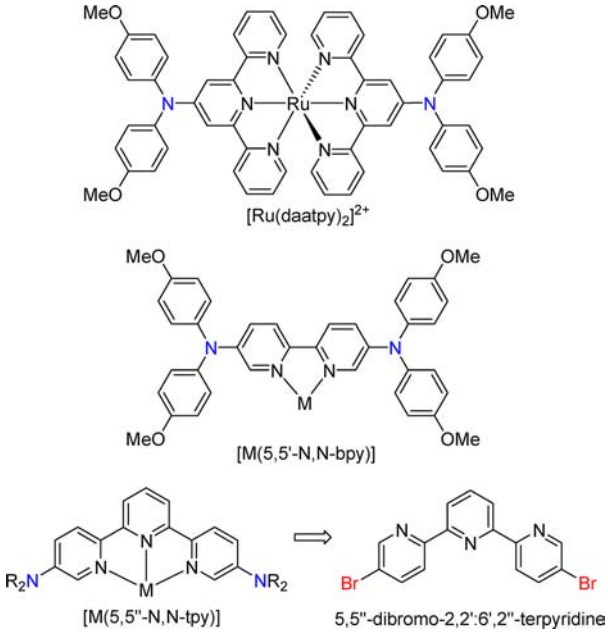

Figure 1. Metal-containing bis-amines. Counteranions have been omitted.

attention to a new compound (Scheme 1), 4′-tolyl-5,5″-dibromo-2,2′:6′,2″-terpyridine (**1**), which can be prepared through a one-step reaction from commercially available sources using a known approach to 4′-aryl-2,2′:6′,2″-terpyridine compounds.[18] Compound **1** was later used to prepare bis-amine ligand **2** and two ruthenium complexes, $\mathbf{3}^{2+}$ and $\mathbf{4}^{2+}$, where complex $\mathbf{4}^{2+}$ contains three redox-active amine sites. In this contribution, we present the electrochemical, optical, and computational studies of these compounds.

RESULTS AND DISCUSSION

Syntheses and Crystal Structures. As shown in Scheme 1, 4′-tolyl-5,5″-dibromo-2,2′:6′,2″-terpyridine (**1**) was prepared by condensation reaction using *p*-tolualdehyde and 2-acetyl-5-bromopyridine in the presence of aqueous ammonia and potassium hydroxide (78% yield).[18] A palladium-catalyzed C–N coupling[19] between **1** and 4,4′-dimethoxydiphenylamine afforded the bis-amine ligand **2** in 36% yield. The reactions of **2** with $[Ru(ttpy)Cl_3]$ and $[Ru(daatpy)Cl_3]$[15] (ttpy = 4′-tolyl-2,2′:6′,2″-terpyridine), followed by anion exchange with KPF_6, yielded complexes $\mathbf{3}^{2+}$ and $\mathbf{4}^{2+}$ in acceptable yield, respectively. The details of synthesis and characterization data are given in the Experimental Section.

A single crystal of $\mathbf{4}^{2+}$ suitable for X-ray analysis[20] was obtained by the slow diffusion of petroleum ether into a solution of $\mathbf{4}^{2+}$ in chloroform. A thermal ellipsoid plot of $\mathbf{4}^{2+}$ is shown in Figure 2. The ruthenium atom has a distorted octahedral configuration. All triarylamine units have a configuration like a three-bladed propeller with a planar central nitrogen atom. The amine unit with the N3 atom in the daatpy ligand is sandwiched between two methoxybenzene rings in the NN ligand but slightly bent toward one of them. However, this slight distortion is not preserved in solution. The ^{1}H NMR spectrum of $\mathbf{4}^{2+}$ (provided in the Supporting Information, SI) is in accordance with a C_2-symmetric chemical structure. For simplicity, the triarylamine on the daatpy ligand will be referred to as central triarylamine and those on the NN ligand with N1 or N2 atoms as peripheral triarylamines.

Scheme 1. Synthesis of Compounds Studied

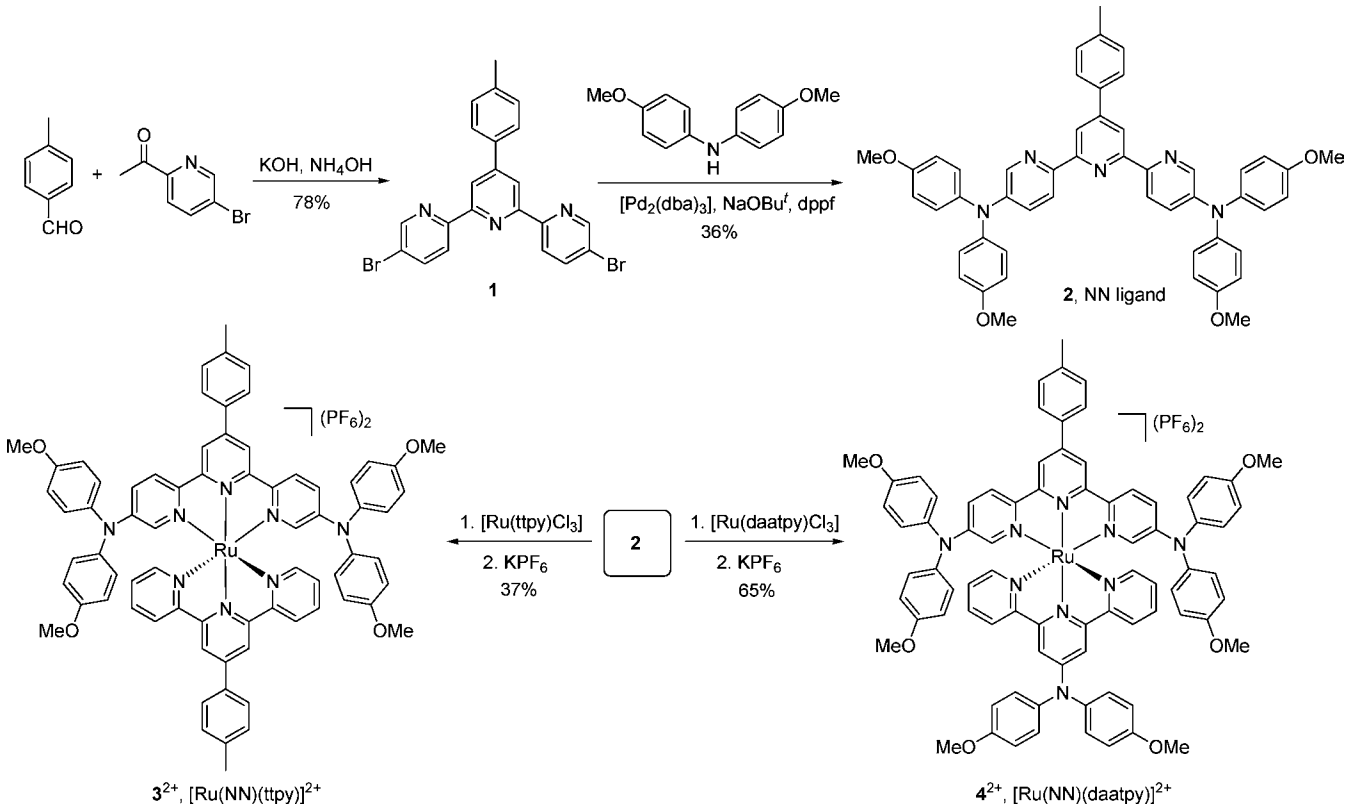

dx.doi.org/10.1021/ic301004e | *Inorg. Chem.* 2012, 51, 11387–11395

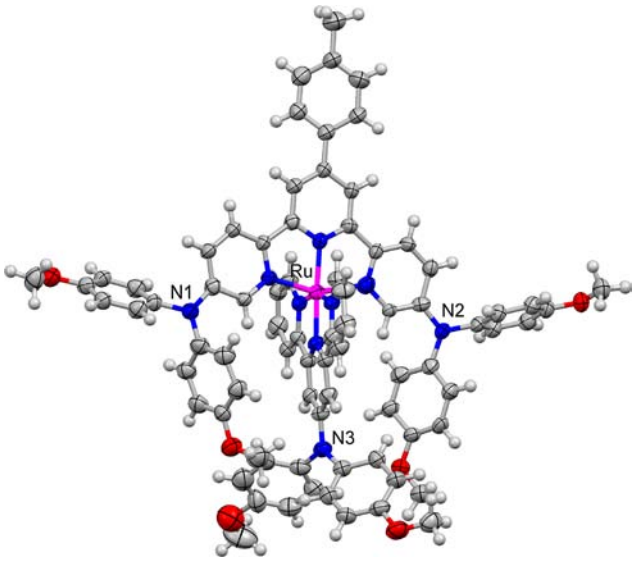

Figure 2. Thermal ellipsoid plot of $[4](PF_6)_2$ with 50% probalility. Solvents and counteranions are omitted for clarity. Atom color code: hydrogen, white gray; carbon, gray; nitrogen, blue; oxygen, red; ruthenium, magenta.

Electrochemical Studies. The electronic properties of bisamine **2** and complexes 3^{2+} and 4^{2+} were examined by electrochemical analysis (Figure 3 and Table 1). Two closely spaced anodic couples at +0.80 and +0.85 V vs Ag/AgCl are evident in the cyclic voltammogram (CV) of ligand **2**, which is also discernible on the Gaussian-fitted curves of its differential pulse voltammogram (DPV; Figure 3a). These waves are assigned to the chemically reversible $N/N^{\bullet+}$ processes of two triarylamine units in ligand **2**. It should be noted that the oxidations assigned to the two amine groups in **2** occur at slightly lower potentials than that of the daatpy ligand (+0.97 V under the same measurement conditions).[15] The irreversible peak at a more positive potential in Figure 3a is due to further oxidation of the in situ produced $N^{\bullet+}$ group ($N^{+/2+}$ process).[21] In the anodic scan of complex 3^{2+}, only a two-electron $N/N^{\bullet+}$ wave is observed at +1.03 V vs Ag/AgCl. The $Ru^{II/III}$ process at +1.44 V overlaps with the irreversible $N^{+/2+}$ processes, which is more evident in the DPV in Figure 3b. Two ligand-based reduction waves at −1.24 and −1.57 V are observed in the cathodic scan of 3^{2+}. The height of each reduction wave is around half that of the anodic couple at +1.03 V, which supports the assertion that the latter one is a two-electron event. The oxidations of the amine units in complex 3^{2+} occur at more positive potentials than those in ligand **2**, reflecting the electron-withdrawing nature of the metal component.

Figure 3c shows the CV and DPV of complex 4^{2+}. Two cathodic couples at −1.37 and −1.67 V vs Ag/AgCl are observed. The anodic peak around +1.0 V is somewhat broad and roughly 3 times as high as each cathodic peak. Besides, two Gaussian-fitted curves at +0.99 and +1.06 V with a 1:2 height ratio can be deconvolved from the DPV band. This makes us believe that the peak at +1.0 V is a three-electron event and is associated with the oxidations of three amine units in 4^{2+}. Considering that the oxidation of the triarylamine in ligand **2** is easier than that in daatpy, the first oxidation event of 4^{2+} is likely associated with one of the peripheral amines of the NN ligand. The irreversible peak at +1.37 V is assigned to the further $N^{+/2+}$ process, followed by the $Ru^{II/III}$ wave at +1.61 V.

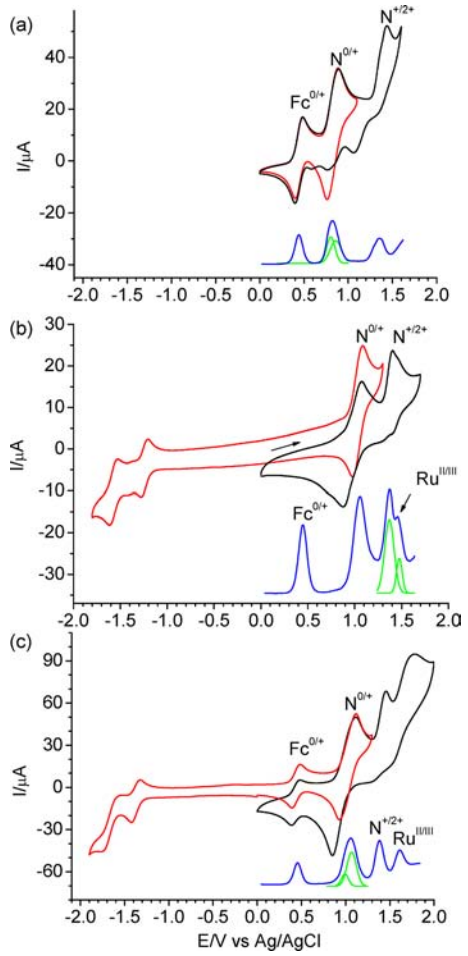

Figure 3. CVs and DPVs (blue lines) of (a) **2**, (b) 3^{2+}, and (c) 4^{2+} in CH_2Cl_2/CH_3CN (1:1) at a scan rate of 100 mV s^{-1} containing ferrocene as an internal standard (except CVs in part b). Green lines represent the Gaussian-fitted curves of some DPV bands.

Table 1. Electrochemical Data

	$E_{1/2}$[a] (anodic)		
compound	amine	$Ru^{II/III}$	$E_{1/2}$[a] (cathodic)
2, NN ligand	+0.80, +0.85, +1.40[b]		
3^{2+}, $[Ru(NN)(ttpy)]^{2+}$	+1.03 (2e), +1.40[b]	+1.44	−1.24, −1.57
4^{2+}, $[Ru(NN)(daatpy)]^{2+}$	+0.99, +1.06 (2e), +1.37[b]	+1.61	−1.37, −1.67
daatpy[c]	+0.97, +1.41[b]		
$[Ru(daatpy)(tpy)]^{2+}$[c]	+0.98, +1.35[b]	+1.44	−1.34, −1.58
$[Ru(tpy)_2]^{2+}$[c]		+1.32	−1.22, −1.46

[a]The potential is reported as the $E_{1/2}$ value vs Ag/AgCl. Potentials vs $Fc^{0/+}$ can be derived by subtracting 0.45 V. [b]$E_{p,anodic}$, irreversible. [c]See ref 15.

It should be noted that the $Ru^{II/III}$ potentials for complexes 3^{2+}, 4^{2+}, and $[Ru(daatpy)(tpy)]^{2+}$ are all more positive than that of the pristine complex $[Ru(tpy)_2]^{2+}$,[15] as a result of the presence of the electron-withdrawing aminium cations.

Density Functional Theory (DFT) Calculations. DFT calculations of complexes 3^{2+} and 4^{2+} were performed on the level of B3LYP/Lanl2DZ/6-31G*/conductor-like polarizable continuum model (CPCM) with the inclusion of solvent (CH_2Cl_2) to aid in the understanding of their electronic structures (see details in the Experimental Section). Figures 4

dx.doi.org/10.1021/ic301004e | Inorg. Chem. 2012, 51, 11387−11395

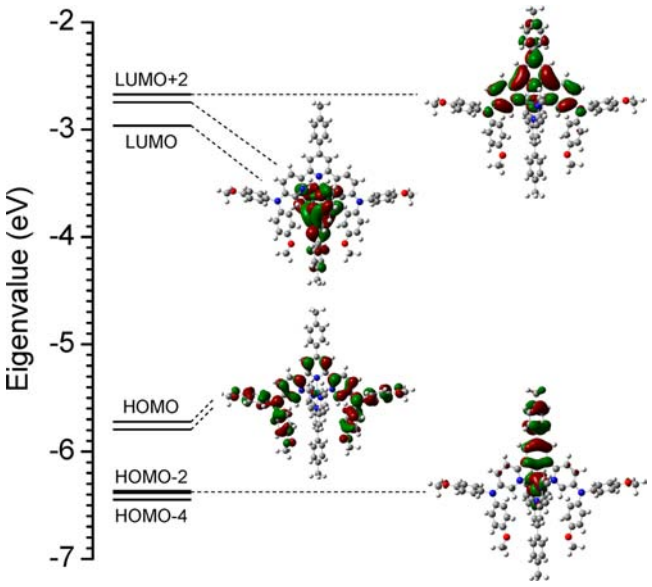

Figure 4. Isodensity plots of selected frontier orbitals for 3^{2+} along with the energy diagram. All orbitals have been computed at the level of B3LYP/Lanl2DZ/6-31G*/CPCM/CH_2Cl_2 with an isovalue of 0.02 e $bohr^{-3}$.

and 5 provide the isodensity plots of selected frontier orbitals along with the energy diagram. More graphics of frontier

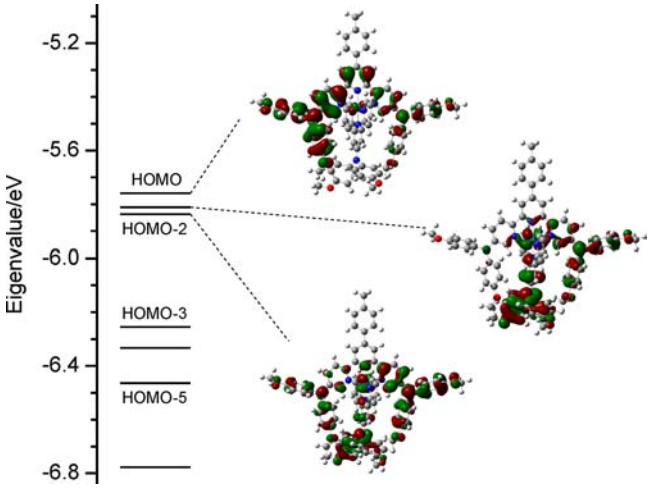

Figure 5. Isodensity plots of selected frontier orbitals for 4^{2+} along with the energy diagram. All orbitals have been computed at the level of B3LYP/Lanl2DZ/6-31G*/CPCM/CH_2Cl_2 with an isovalue of 0.02 e $bohr^{-3}$.

orbitals are given in Figures S1 and S2 in the SI. The lowest unoccupied molecular orbital (LUMO) and LUMO+1 of 3^{2+} are associated with the ttpy ligand. A higher-lying LUMO+2 is dominated by the NN ligand. This information is helpful for the assignment of the cathodic electrochemical waves in Figure 3b, where reduction of the ttpy ligand in complex 3^{2+} occurs prior to the bis-amine ligand. The highest occupied molecular orbital (HOMO) and HOMO−1 of 3^{2+} have similar configurations, dominated by two triarylamine units. They are well-separated from the lower-lying metal-associated occupied orbitals, such as HOMO−2, HOMO−3, and HOMO−4.

The configurations of the first few unoccupied frontier orbitals of complex 4^{2+} are very similar to those of 3^{2+}. The daatpy ligand contributes dominantly to the LUMO and LUMO+1. The NN ligand is responsible for the LUMO+2 level (Figure S2 in the SI). Accordingly, the cathodic CV waves at −1.37 and −1.67 V in Figure 3c are assigned to reduction of the daatpy and NN ligands in complex 4^{2+}, respectively. The HOMO of 4^{2+} is associated with two peripheral triarylamines but biased toward one of them. The HOMO−1 has contributions from the central triarylamine and one of the peripheral amines. All three amines contribute to the HOMO−2 level. The calculated energy separations among these orbitals are relatively small ($\Delta E_{HOMO/HOMO-1}$ = 0.06 eV; $\Delta E_{HOMO-1/HOMO-2}$ = 0.03 eV), which indeed correlates well with the above electrochemical results of 4^{2+} that show the oxidations of three triarylamines around similar potentials. Lower-lying occupied orbitals of 4^{2+}, such as HOMO−3, HOMO−4, and HOMO−5, are mainly associated with the metal component.

Spectroscopic Studies and Time-Dependent DFT (TDDFT) Calculations. Absorption spectra of 3^{2+} and 4^{2+} were recorded and paralleled by TDDFT calculations. Experimental spectra are shown in Figure 6, together with

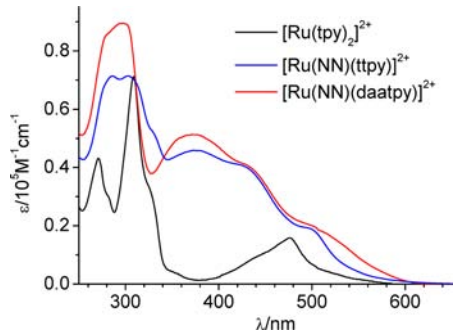

Figure 6. (a) UV/vis absorption spectra of $[Ru(NN)(ttpy)](PF_6)_2$ (3^{2+}), $[Ru(NN)(daatpy)](PF_6)_2$ (4^{2+}), and $[Ru(tpy)_2](PF_6)_2$ in CH_2Cl_2.

that of $[Ru(tpy)_2]^{2+}$. Predicted excitations are given in Table S1 and Figure S3 in the SI. Frontier orbitals involved in these excitations are given in Figures S1 and S2 in the SI. Complexes 3^{2+} and 4^{2+} absorb continuously from the ultraviolet (UV) to the visible region. Clearly, light absorption of 3^{2+} and 4^{2+} is much more enhanced than the prototype compound $[Ru(tpy)_2](PF_6)_2$, in both terms of strength and width.

In the visible region for 3^{2+}, two shoulder bands around 430 and 500 nm can be discerned. According to TDDFT results, the latter band is mainly associated with the S_4 excitation, which is dominated by the HOMO → LUMO+2 intraligand charge-transfer (ILCT) transitions. However, the former band should be interpreted as a result of both ILCT and MLCT transitions, mainly associated with S_9, S_{12}, S_{13}, and S_{16} excitations. A very shallow shoulder band around 530 nm can also be discerned for complex 4^{2+}. TDDFT results predict that S_2, S_3, S_4, and S_6 excitations are responsible for this band and they are largely of ILCT and ligand-to-ligand-charge-transfer (LLCT) origin from three triarylamine units. In the region between 400 and 450 nm, TDDFT results imply the presence of a set of complex excitations (from S_{12} to S_{18}) with mixed contributions from MLCT, LLCT, and ILCT transitions. These excitations are responsible for the absorption bands experimentally observed between 340 and 480 nm for complex 4^{2+}

dx.doi.org/10.1021/ic301004e | Inorg. Chem. 2012, 51, 11387−11395

Oxidative Titration and Near-Infrared (NIR) Transition Analysis. In the studies of triarylamine mixed-valence systems, a routine method is used to stepwisely oxidize individual amine units, using a chemical (for instance, a solution of $SbCl_5$ in CH_2Cl_2)[22] or an electrochemical method, and to monitor the NIR spectral changes to see if an IVCT band can be observed.[13] Because of the possible complexity caused by coordination of the tpy ligand to $SbCl_5$, an electrochemical method is preferred for the bis-amine ligand **2**. When a solution of **2** in CH_2Cl_2 was subjected to oxidative electrolysis on an indium−tin oxide (ITO) glass electrode (the potential was gradually applied from +0.4 to +1.2 V vs Ag/AgCl; see details in the Experimental Section), the ILCT band at 377 nm gradually decreased, with the concomitant appearance of two new bands at 490 and 780 nm (Figure 7). This indicates generation of a nitrogen radical

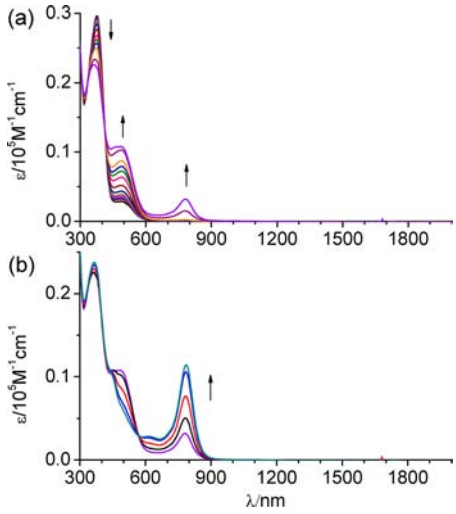

Figure 7. Absorption spectral changes of the bis-amine ligand **2** in CH_2Cl_2 upon (a) a first one-electron and (b) a second one-electron oxidation by stepwise oxidative electrolysis at an ITO glass.

cation group ($N^{\bullet+}$) in the solution. The appearance of two similar bands for the $N^{\bullet+}$ group in this region has previously been documented.[12,23] Upon a further increase in the potential to +1.2 V, the peak at 780 nm increased continuously and no more absorption bands were observable in the NIR region during the oxidation process. Figure 8 shows the NIR spectral changes of complex 3^{2+} upon the gradual addition of up to 2 equiv of $SbCl_5$ in CH_2Cl_2. Similarly, the absorption bands around 400 nm were found to decrease, and two new bands at

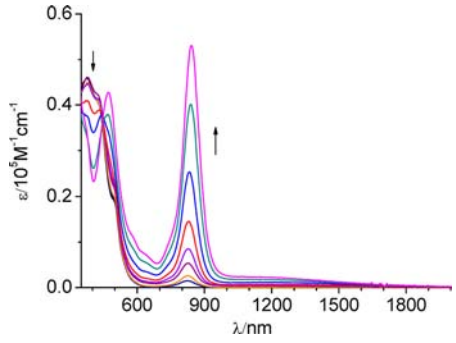

Figure 8. Absorption spectral changes of 3^{2+} in CH_2Cl_2 upon two-electron oxidation by the gradual addition of $SbCl_5$.

470 and 840 nm due to the $N^{\bullet+}$ group developed. The shallow low-energy band between 1000 and 1800 nm is very likely due to the charge-transfer transition from the metal center to the generated $N^{\bullet+}$ group.[15] It is clear from Figures 7 and 8 that no IVCT band is observable for **2** and 3^{2+} during the oxidation process, which indicates that the electronic coupling between two amines in these compounds is very weak. The emergence of the $N^{\bullet+}$-associated absorption around 800 nm of 3^{2+} upon oxidation can also be observed through electrolysis at an ITO glass electrode (Figure S4 in the SI, applying a potential from +0.70 to +1.10 V vs Ag/AgCl). However, this band is much weaker than that observed in Figure 8 upon chemical oxidation. Upon a further increase in the potential, this band began to decrease, indicating decomposition of the in situ generated $N^{\bullet+}$ group. Thus, for studies of triarylamine-containing complexes with a relatively high $N^{0/+}$ potential, chemical oxidation is preferred.

The spectral changes for complex 4^{2+} with three redox-active amine sites upon oxidative titration are significantly different from those for **2** and 3^{2+}. When a proper amount of $SbCl_5$ (around 2 equiv) was gradually added to a solution of 4^{2+}, a new peak at 1430 nm with medium intensity increased along with the emergence of a $N^{\bullet+}$-associated absorption at 820 nm (Figure 9a). Upon a further increase in the amount of $SbCl_5$,

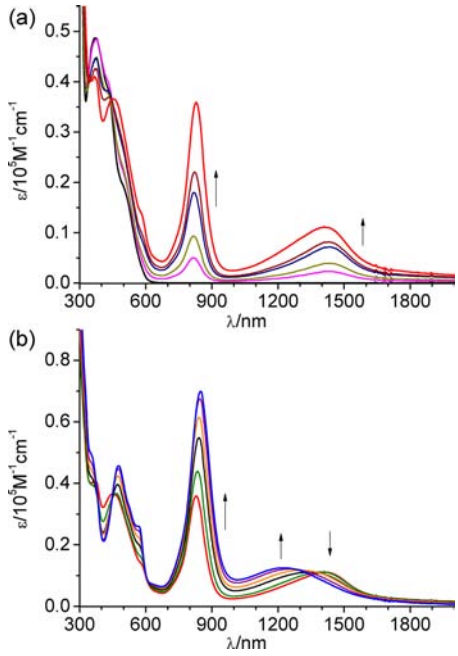

Figure 9. Absorption spectral changes of 4^{2+} in CH_2Cl_2 upon (a) single and (b) double oxidation by the gradual addition of $SbCl_5$.

the peak at 1430 nm decreased but the $N^{\bullet+}$-associated absorption continued to increase. At the same time, the appearance of another new peak at 1220 nm was observed (Figure 9b). When an excess of the oxidant was added, no more changes were evident.

Taking into account the above electrochemical and DFT results and the oxidative titration measurements, we believe that the peripheral triarylamines of the NN ligand of 4^{2+} were first oxidized, followed by the oxidation of the central amine of the daatpy ligand. In the singly and doubly oxidized forms (4^{3+} and 4^{4+}), the peak at 1430 nm is ascribed to the LLCT ($N \rightarrow N'^{\bullet+}$) transitions from the neutral central amine to the oxidized

dx.doi.org/10.1021/ic301004e | Inorg. Chem. 2012, 51, 11387−11395

peripheral aminium units. In the triply oxidized form, the peak at 1220 nm is assigned to a MLCT ($M \rightarrow N^{\bullet+}$) band associated with the oxidized central aminium unit in the daatpy ligand. This assignment is reasonable considering the fact that an intense $Ru \rightarrow N^{\bullet+}$ MLCT band at 1360 nm has been previously[15] observed for the monooxidized form of $[Ru(daatpy)(tpy)]^{2+}$, while the singly oxidized $\mathbf{3}^{3+}$ only displayed very weak and shallow bands in the region with wavelength longer than 1000 nm.

Assuming symmetric shapes, the NIR bands for the doubly oxidized state of $\mathbf{4}^{2+}$ with $\lambda > 1000$ nm were deconvolved into two Gaussian-fitted bands at 8400 and 7140 cm^{-1} (pink and blue lines, respectively, in Figure 10). The latter band is the N

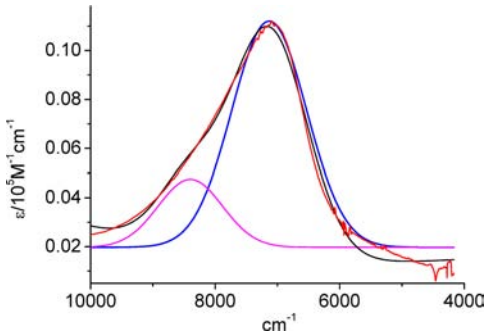

Figure 10. Gaussian-fitted curves of the NIR bands for the doubly oxidized form of $\mathbf{4}^{2+}$. The red line shows the experimental data. The blue and pink lines are Gaussian-fitted curves of the experimental data. The black line stands for the sum of the blue and pink lines.

$\rightarrow N'^{\bullet+}$ LLCT transition, while the former band is very likely of the $Ru \rightarrow N^{\bullet+}$ MLCT origin, as has been discussed above. The LLCT band has ε_{max} of 11000 M^{-1} cm^{-1} and $\Delta\nu_{1/2}$ of 1600 cm^{-1}. If the Hush formula[24] $H_{NN} = 0.0206(\varepsilon_{max}\nu_{max}\Delta\nu_{1/2})^{1/2}/r_{ab}$ is used and the average geometrical distance between the central amine and each peripheral amine site is taken as the electron-transfer distance, a H_{NN} value of 1000 cm^{-1} can be deduced. However, because these data were obtained from the doubly oxidized form, the coupling parameter H_{NN} associated with each amine site should be half of the calculated H_{NN} value. In addition, this value should only be taken as a rough estimate because the real electron-transfer distance is unknown.[25] The nature of the underlying electron-transfer process could be complex. Considering the space proximity between the peripheral and central amine units, the involvement of a through-space process is possible.[26] However, a charge transfer involving some hybrid oribtals containing the central ruthenium site is also possible.

In many studies on mixed-valence systems, DFT and TDDFT calculations were performed on the open-shell substances to provide insight into the spin-density distribution and the nature of IVCT bands.[27] Using the same method (B3LYP/Lanl2DZ/6-31G*/CPCM), we have carried out similar calculations on the basis of the previously DFT-optimized structure of $\mathbf{4}^{2+}$ after changing the charge to 3+ and spin multiplicity to 2. The spin density is dominated by one peripheral triarylamine in the NN ligand, which is consistent with the above interpretations that one peripheral amine is oxidized first and behaves as the acceptor for the $N \rightarrow N^{\bullet+}$ LLCT transitions (Figure 11). TDDFT calculations have also been performed on the optimized structure of $\mathbf{4}^{3+}$ in CH_2Cl_2. Predicted excitations are summarized in Table S2 in the SI, and

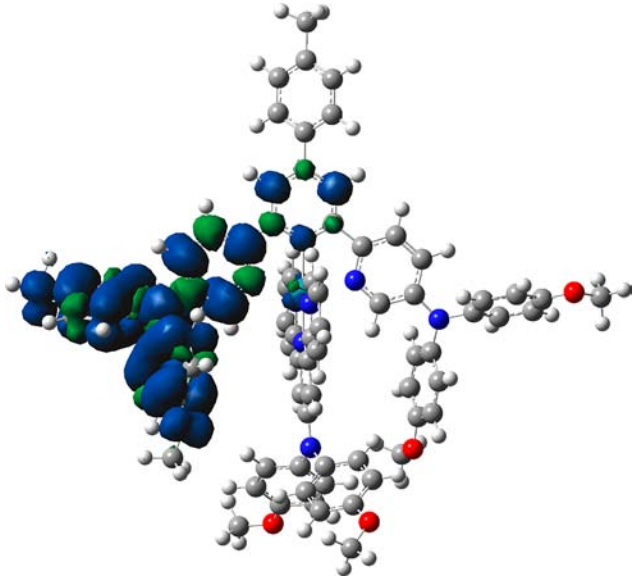

Figure 11. DFT-calculated spin-density distribution of $\mathbf{4}^{3+}$ at the level of B3LYP/Lanl2DZ/6-31G*/CPCM/CH_2Cl_2.

involved frontier spin orbitals are shown in Figure S5 in the SI. However, the computed predictions do not fully agree with the above spectroscopic assignment. For instance, $N \rightarrow N^{\bullet+}$ LLCT transitions are predicted to be at a very low-energy region (around 3000 nm) associated with the 332B $\rightarrow$ 333B and 331B $\rightarrow$ 333B excitations (S_1 and S_2). The S_3 and S_4 excitations from 330B and 329B orbitals may correlate with the experimentally observed $Ru \rightarrow N^{\bullet+}$ MLCT transitions at 1220 nm. In addition, the $N^{\bullet+}$-group-associated absorption band at 850 nm in Figure 9b can be explained by the predicted S_8 excitation with the 324B $\rightarrow$ 333B origin.

CONCLUSION

Compounds with multiple redox sites can be treated as a special class of mixed-valence systems,[26] where a multichannel charge-transfer pathway is possible. We present in this paper two new bis-amine compounds, **2** and $\mathbf{3}^{2+}$, and one ruthenium complex, $\mathbf{4}^{2+}$, containing three redox-active amine sites. The amine–amine electronic coupling through the 5 and 5″ positions of 2,2′:6′,2″-terpyridine was proven to be insignificant, either in the presence of a laterally chelated metal component or not. However, an effective charge transfer occurred from the central neutral amine of the daatpy ligand of $\mathbf{4}^{2+}$ to an oxidized aminium cation of another ligand of the same complex. These findings demonstrated that the $[Ru(tpy)_2]$ core could be used to effectively mediate an electronic coupling between redox sites attached on individual ligands. DFT and TDDFT calculations provided some useful information on the electronic properties of compounds studied. The attachment of triaryl-amine units to the $[Ru(tpy)_2]$ core was proven to be efficient for the enhancement of light absorption, as has been reported in published works.[9,15,16] This feature will make these hybrid materials useful in some optoelectronic applications.[6,10]

EXPERIMENTAL SECTION

Spectroscopic Measurement. All optical UV/vis absorption spectra were obtained using a TU-1810DSPC spectrometer from Beijing Purkinje General Instrument Co. Ltd. at room temperature in the solvents noted, with a conventional 1.0 cm quartz cell. UV/vis/NIR spectra were recorded using a PE Lambda 750 UV/vis/NIR

spectrophotometer. Oxidative spectroelectrochemistry was performed in a thin-layer cell (optical length 0.2 cm) in which an ITO glass electrode was set in the indicated solvent containing the compound to be studied (the concentration is around 1×10^{-4} M) with 0.1 M Bu_4NClO_4 as the supporting electrolyte. A platinum wire and Ag/AgCl in a saturated aqueous NaCl solution were used as counter and reference electrodes, respectively. The cell was put into the spectrophotometer to monitor spectral changes during electrolysis.

Electrochemical Measurement. All CV measurements were taken using a CHI620D potentiostat with a one-compartment electrochemical cell under an atmosphere of nitrogen. All measurements were carried out in denoted solvents containing 0.1 M $^nBu_4NClO_4$ as the supporting electrolyte at a scan rate of 100 mV s^{-1}. The working electrode was a glassy carbon with a diameter of 0.3 mm. The electrode was polished prior to use with 0.05 μm alumina and rinsed thoroughly with water and acetone. A large-area platinum wire coil was used as the counter electrode. All potentials are referenced to a Ag/AgCl electrode in saturated aqueous NaCl without regard for the liquid junction potential.

X-ray Crystallography. A single crystal of $[4](PF_6)_2$ was mounted on a glass fiber and transferred into the cold nitrogen stream. The X-ray diffraction data were collected using a Rigaku Saturn 724 diffractometer on a rotating anode (Mo Kα radiation, λ = 0.71073 Å). The structure was solved by direct methods using *SHELXS-97* and refined anisotropically on F^2 with *SHELXL-97*.[28] All hydrogen atoms were located in their idealized positions, with a methyl C−H bond length of 0.98 Å and an aromatic C−H bond length of 0.95 Å, and included in the refinement using a riding model approximation.

Computational Methods. DFT and TDDFT calculations are carried out using the B3LYP exchange correlation functional[29] and implemented in the *Gaussian 03* program package.[30] The electronic structures of complexes were determined using a general basis set with the Los Alamos effective core potential LanL2DZ basis set for ruthenium and 6-31G* for other atoms.[31] Solvent effects (CH_2Cl_2) are included in all calculations with the CPCM.[32]

Synthesis of 5,5′-Dibromo-4′-tolyl-2,2′:6′,2″-terpyridine (1). To 20 mL of dry ethanol were added potassium hydroxide (336 mg, 4.0 mmol), *p*-tolualdehyde (0.36 mL, 3.0 mmol), 2-acetyl-5-bromopyridine (1.2 g, 6.0 mmol), and 9 mL of a 25% aqueous ammonia solution. After stirring for 8 h at room temperature, the resulting precipitate was collected after filtration, and the crude product was purified through flash column chromatography on silica gel (eluent: 15:1 petroleum ether/ethyl acetate) to afford 1.13 g of **1** as a white solid in a yield of 78%. ^{1}H NMR (400 MHz, $CDCl_3$): δ 2.44 (s, 3H), 7.33 (d, J = 7.9 Hz, 2H), 7.79 (d, J = 7.9 Hz, 2H), 7.97 (d, J = 8.5 Hz, 2H), 8.52 (d, J = 8.5 Hz, 2H), 8.70 (s, 2H), 8.76 (s, 2H). ^{13}C NMR (100 MHz, $CDCl_3$): δ 21.3, 118.7, 121.2, 122.5, 127.0, 129.7, 135.1, 139.4, 150.1, 150.2, 154.6, 154.9. EI-MS: m/z 481 ($[M]^+$). Anal. Calcd for $C_{22}H_{15}Br_2N_3$: C, 54.91; H, 3.14; N, 8.73. Found: C, 55.11; H, 3.29; N, 8.64.

Synthesis of 5,5′-Bis(di-*p*-anisylamino)-4′-tolyl-2,2′:6′,2″-terpyridine (2). To a 100-mL oven-dried pressure vessel were added **1** (0.5 mmol, 241 mg), 4,4′-dimethoxydiphenylamine (1.5 mmol, 344 mg), and 25 mL of dry toluene. The solution was bubbled with nitrogen for 10 min, followed by the addition of $[Pd_2(dba)_3]$ (0.033 mmol, 30 mg), dppf (0.036 mmol, 20 mg), and $NaOBu^t$ (1.87 mmol, 180 mg). The vessel was sealed, and the mixture was stirred at 140 °C for 48 h. After cooling to room temperature, the solvent was removed under reduced pressure. The residue was subjected to flash column chromatography on silica gel (eluent: 4:1 petroleum ether/acetone) to afford 140 mg of **2** as a yellow solid in a yield of 36%. ^{1}H NMR (400 MHz, $CDCl_3$): δ 2.40 (s, 3H), 3.81 (s, 12H), 6.87 (d, J = 8.8 Hz, 8H), 7.11 (d, J = 8.8 Hz, 8H), 7.27 (d, J = 8.4 Hz, 2H), 7.34 (dd, J = 8.8 and 2.6 Hz, 2H), 7.77 (d, J = 7.9 Hz, 2H), 8.31 (d, J = 2.0 Hz, 2H), 8.39 (d, J = 8.8 Hz, 2H), 8.50 (s, 2H). MALDI-MS: m/z 778.5 ($[M]^+$). Anal. Calcd for $C_{50}H_{43}N_5O_4 \cdot 0.5H_2O$: C, 76.32; H, 5.64; N, 8.90. Found: C, 76.38; H, 5.67; N, 8.56.

Synthesis of Complex [3](PF$_6$)$_2$. To 5 mL of ethylene glycol were added ligand **2** (0.056 mmol, 44 mg) and $[Ru(ttpy)Cl_3]$ (0.056 mmol, 30 mg). The mixture was heated to reflux under microwave heating (power = 375 W) for 30 min. After cooling to room temperature, 200 mg of KPF_6 dissolved in 5 mL of water was added. The resulting precipitate was collected by filtration and washing successively with water and ether. The crude product was subjected to column chromatography on silica gel (eluent: 20:1 CH_2Cl_2/CH_3CN) to afford 31 mg of $[3](PF_6)_2$ as a reddish-brown solid in a yield of 37%. ^{1}H NMR (400 MHz, CD_3CN): δ 2.50 (s, 3H), 2.57 (s, 3H), 3.55 (s, 12H), 6.43 (d, J = 2.4 Hz, 2H), 6.77 (s, 16H), 7.05 (dd, J = 9.1 and 2.5 Hz, 2H), 7.28 (t, J = 6.5 Hz, 2H), 7.46 (d, J = 8.2 Hz, 2H), 7.52 (d, J = 7.9 Hz, 2H), 7.59 (d, J = 7.8 Hz, 2H), 7.95 (d, J = 7.9 Hz, 2H), 8.02 (m, 4H), 8.17 (d, J = 9.2 Hz, 2H), 8.56 (s, 2H), 8.60 (d, J = 7.5 Hz, 2H), 8.61 (s, 2H). MALDI-MS: m/z 1202.1 ($[M - 2PF_6]^+$). Anal. Calcd for $C_{72}H_{60}F_{12}N_8O_4P_2Ru \cdot H_2O$: C, 57.26; H, 4.14; N, 7.42. Found: C, 57.00; H, 4.05; N, 7.18.

Synthesis of Complex [4](PF$_6$)$_2$. To 5 mL of ethylene glycol were added ligand **2** (0.048 mmol, 37 mg) and $[Ru(daatpy)Cl_3]$ (0.06 mmol, 39 mg). The mixture was heated to reflux under microwave heating (power = 375 W) for 30 min. After cooling to room temperature, 100 mg of KPF_6 dissolved in 5 mL of water was added. The resulting precipitate was collected by filtration and washing successively with water and ether. The crude product was subjected to column chromatography on silica gel (eluent: 200:1:20 acetone/saturated aqueous KNO_3/water) to afford 52 mg of complex $[4](PF_6)_2$ as a reddish-brown solid in a yield of 65%. ^{1}H NMR (400 MHz, CD_3CN): δ 2.49 (s, 3H), 3.77 (s, 12H), 3.90 (s, 6H), 6.75 (d, J = 2.4 Hz, 2H), 6.84 (dd, J = 8, 8 Hz, 16H), 7.03 (d, J = 9.2 Hz, 2H), 7.14−7.16 (m, 10H), 7.20 (d, J = 8.4 Hz, 2H), 7.36 (d, J = 5.2 Hz, 2H), 7.49 (s, 2H), 7.62 (t, J = 8 Hz, 2H), 7.99 (d, J = 8.4 Hz, 2H), 8.08 (d, J = 8 Hz, 2H), 8.15 (d, J = 8.8 Hz, 2H), 8.52 (s, 2H). MALDI-MS: m/z 1338.4 ($[M - 2PF_6]^+$). Anal. Calcd for $C_{79}H_{67}F_{12}N_9O_6P_2Ru \cdot 2H_2O$: C, 56.97; H, 4.30; N, 7.57. Found: C, 56.90; H, 4.19; N, 7.60.

■ ASSOCIATED CONTENT

Supporting Information

Frontier orbital graphics, DFT-optimized Cartesian coordinates, TDDFT results, ^{1}H NMR and MS spectra of new compounds, and a CIF file for a single crystal of $[4](PF_6)_2$. This material is available free of charge via the Internet at http://pubs.acs.org.

■ AUTHOR INFORMATION

Corresponding Author

*E-mail: zhongyuwu@iccas.ac.cn.

Author Contributions

§These authors contributed equally.

Notes

The authors declare no competing financial interest.

■ ACKNOWLEDGMENTS

We thank the National Natural Science Foundation of China (Grants 21271176 and 21002104), the National Basic Research 973 program of China (Grant 2011CB932301), and Institute of Chemistry, Chinese Academy of Sciences ("100 Talent" Program and Grant CMS-PY-201230), for funding support.

■ REFERENCES

(1) (a) Barigelletti, F.; Flamigni, L. *Chem. Soc. Rev.* **2000**, *29*, 1. (b) Balzani, V.; Juris, A. *Coord. Chem. Rev.* **2001**, *211*, 97. (c) Schubert, U. S.; Eschbaumer, C. *Angew. Chem., Int. Ed.* **2002**, *41*, 2892. (d) Baranoff, E.; Collin, J.-P.; Flamigni, L.; Sauvage, J.-P. *Chem. Soc. Rev.* **2004**, *33*, 147. (e) Medlycott, E. A.; Hanan, G. S. *Chem. Soc. Rev.* **2005**, *34*, 133. (f) Constable, E. C. *Chem. Soc. Rev.* **2007**, *36*, 246. (g) Eryazici, I.; Moorefield, C. N.; Newkome, G. R. *Chem. Rev.* **2008**, *108*, 1834.

(2) (a) Evans, R. C.; Douglas, P.; Winscom, C. J. *Coord. Chem. Rev.* **2006**, *250*, 2093. (b) Slinker, J. D.; Rivnay, J.; Moskowitz, J. S.; Parker, J. B.; Bernard, S.; Abruña, H. D.; Malliaras, G. G. *J. Mater. Chem.* **2007**, *17*, 2976.
(3) (a) Abbotto, A.; Manfredi, N. *Dalton Trans.* **2011**, *40*, 12421. (b) Reynal, A.; Palomares, E. *Eur. J. Inorg. Chem.* **2011**, 4509.
(4) (a) D'Alessandro, D. M.; Keene, F. R. *Chem. Rev.* **2006**, *106*, 2270. (b) Kaim, W.; Lahiri, G. K. *Angew. Chem., Int. Ed.* **2007**, *46*, 1778. (c) Aguirre-Etcheverry, P.; O'Hare, D. *Chem. Rev.* **2010**, *110*, 4839. (d) Low, P. J.; Brown, N. J. *J. Cluster Sci.* **2010**, *21*, 235. (e) Chisholm, M. H.; Lear, B. J. *Chem. Soc. Rev.* **2011**, *40*, 5254. (f) Xi, B.; Liu, I. P.-C.; Xu, G.-L.; Choudhuri, M. M. R.; DeRosa, M. C.; Crutchley, R. J.; Ren, T. *J. Am. Chem. Soc.* **2011**, *133*, 15094. (g) Glover, S. D.; Kubiak, C. P. *J. Am. Chem. Soc.* **2011**, *133*, 8721. (h) Fox, M. A.; Le Guennic, B.; Roberts, R. L.; Brue, D. A.; Yufit, D. S.; Howard, J. A. K.; Manca, G.; Halet, J.-F.; Hartl, F.; Low, P. J. *J. Am. Chem. Soc.* **2011**, *133*, 18433. (i) Yang, W.-W.; Yao, J.; Zhong, Y.-W. *Organometallics* **2012**, *31*, 1035. (j) Yao, C.-J.; Sui, L.-Z.; Xie, H.-Y.; Xiao, W.-J.; Zhong, Y.-W.; Yao, J. *Inorg. Chem.* **2010**, *49*, 8347. (k) Wang, L.; Yang, W.-W.; Zheng, R.-H.; Shi, Q.; Zhong, Y.-W.; Yao, J. *Inorg. Chem.* **2011**, *50*, 7074. (l) Yao, C.-J.; Zhong, Y.-W.; Yao, J. *J. Am. Chem. Soc.* **2011**, *133*, 15697.
(5) (a) Kaim, W. *Coord. Chem. Rev.* **2011**, *255*, 2503. (b) Yao, C.-J.; Zhong, Y.-W.; Nie, H.-J.; Abruña, H. D.; Yao, J. *J. Am. Chem. Soc.* **2011**, *133*, 20720. (c) Yao, C.-J.; Yao, J.; Zhong, Y.-W. *Inorg. Chem.* **2012**, *51*, 6259.
(6) (a) Shirota, Y.; Kageyama, H. *Chem. Rev.* **2007**, *107*, 953. (b) Ning, Z.; Tian, H. *Chem. Commun.* **2009**, 5483.
(7) (a) Scherf, U.; List, E. J. W. *Adv. Mater.* **2002**, *14*, 477. (b) Duan, L.; Hou, L.; Lee, T.-W.; Qiao, J.; Zhang, D.; Dong, G.; Wang, L.; Qiu, Y. *J. Mater. Chem.* **2010**, *20*, 6392.
(8) (a) Cremer, J.; Bäuerle, P.; Wienk, M. M.; Janssen, R. A. J. *Chem. Mater.* **2006**, *18*, 5832. (b) Roquet, S.; Cravino, A.; Leriche, P.; Aleveque, O.; Frere, P.; Roncali, J. *J. Am. Chem. Soc.* **2006**, *128*, 3459.
(9) (a) Li, H.-Y.; Wu, J.; Zhou, X.-H.; Kang, L.-C.; Li, D.-P.; Sui, Y.; Zhou, Y.-H.; Zheng, Y.-X.; Zuo, J.-L.; You, X.-Z. *Dalton Trans.* **2009**, 10563. (b) Sun, Y.; Wang, S. *Inorg. Chem.* **2009**, *48*, 3755. (c) Yao, C.-J.; Zheng, R.-H.; Shi, Q.; Zhong, Y.-W.; Yao, J. *Chem. Commun.* **2012**, *48*, 5680.
(10) (a) Handa, S.; Wietasch, H.; Thelakkat, M.; Durrant, J. R.; Haque, S. A. *Chem. Commun.* **2007**, 1725. (b) Robson, K. C. D.; Koivisto, B. D.; Gordon, T. J.; Baumgartner, T.; Berlinguette, C. P. *Inorg. Chem.* **2010**, *49*, 5335. (c) Robson, K. C. D.; Sporinova, B.; Koivisto, B. D.; Schott, E.; Brown, D. G.; Berlinguette, C. P. *Inorg. Chem.* **2011**, *50*, 6019. (d) Ji, Z.; Li, Y.; Pritchett, T. M.; Makarov, N. S.; Haley, J. E.; Li, Z.; Drobizhev, M.; Rebane, A.; Sun, W. *Chem.—Eur. J.* **2011**, *17*, 2479.
(11) Leung, M.-k.; Chou, M.-Y.; Su, Y. O.; Chiang, C. L.; Chen, H.-L.; Yang, C. F.; Yang, C.-C.; Lin, C.-C.; Chen, H.-T. *Org. Lett.* **2003**, *5*, 839.
(12) Adugna, S.; Revunova, K.; Djukic, B.; Gorelsky, S. I.; Jenkins, H. A.; Lemaire, M. T. *Inorg. Chem.* **2010**, *49*, 10183.
(13) (a) Hankache, J.; Wenger, O. S. *Chem. Rev.* **2011**, *111*, 5138. (b) Heckmann, S.; Lambert, C. *Angew. Chem., Int. Ed.* **2012**, *51*, 326. (c) Lambert, C.; Nöll, G. *J. Am. Chem. Soc.* **1999**, *121*, 8434. (d) Lambert, C.; Nöll, G.; Schelter, J. *Nat. Mater.* **2002**, *1*, 69. (e) Barlow, S.; Risko, C.; Chung, S.-J.; Tucker, N. M.; Coropceanu, V.; Jones, S. C.; Levi, Z.; Brédas, J.-L.; Marder, S. R. *J. Am. Chem. Soc.* **2005**, *127*, 16900. (f) Barlow, S.; Risko, C.; Coropceanu, V.; Tucker, N. M.; Jones, S. C.; Levi, Z.; Khrustalev, V. N.; Antipin, M. Y.; Kinniburgh, T. L.; Timofeeva, T.; Marder, S. R.; Brédas, J.-L. *Chem. Commun.* **2005**, 764. (g) Lacroix, J. C.; Chane-Ching, K. I.; Maquere, F.; Maurel, F. *J. Am. Chem. Soc.* **2006**, *128*, 7264. (h) Amthor, S.; Lambert, C. *J. Phys. Chem. A* **2006**, *110*, 1177. (i) Kattnig, D. R.; Mladenova, B.; Grampp, G.; Kaiser, C.; Heckmann, A.; Lambert, C. *J. Phys. Chem. C* **2009**, *113*, 2983. (j) Sakamoto, R.; Sasaki, T.; Honda, N.; Yamamura, T. *Chem. Commun.* **2009**, 5156. (k) Völker, S. F.; Renz, M.; Kaupp, M.; Lambert, C. *Chem.—Eur. J.* **2011**, *17*, 14147. (l) He, B.; Wenger, O. S. *J. Am. Chem. Soc.* **2011**, *133*, 17027.
(14) (a) Jones, S. C.; Coropceanu, V.; Barlow, S.; Kinnibrugh, T.; Timofeeva, T.; Brédas, J.-L.; Marder, S. R. *J. Am. Chem. Soc.* **2004**, *126*, 11782. (b) Ramírez, C. L.; Pegoraro, C. N.; Filevich, O.; Bruttomeso, A.; Etchenique, R.; Parise, A. R. *Inorg. Chem.* **2012**, *51*, 1261.
(15) Yao, C.-J.; Yao, J.; Zhong, Y.-W. *Inorg. Chem.* **2011**, *50*, 6847.
(16) (a) Nie, H.-J.; Yao, C.-J.; Yao, J.; Zhong, Y.-W. *Chem.—Asian J.* **2011**, *6*, 3322. (b) Nie, H.-J.; Chen, X.; Yao, C.-J.; Zhong, Y.-W.; Hutchison, G. R.; Yao, J. *Chem.—Eur. J.* **2012**, DOI: 10.1002/chem.201201813.
(17) Colasson, B. C.; Dietrich-Buchecker, C.; Sauvage, J.-P. *Synlett* **2002**, 271.
(18) Wang, J.; Hanan, G. S. *Synlett* **2005**, 1251.
(19) Yang, J.-S.; Lin, Y.-H.; Yang, C.-S. *Org. Lett.* **2002**, *4*, 777.
(20) Crystallographic data for $[4](PF_6)_2$: $C_{79}H_{67}N_9O_6RuF_{12}P_2$, M = 1629.43, monoclinic, space group $P2(1)/c$, a = 14.385(3) Å, b = 21.304(4) Å, c = 29.448(6) Å, α = 90°, β = 90.19(3)°, γ = 90°, U = 8909(3) Å^3, T = 173 K, Z = 4, 42614 reflections measured, radiation type Mo Kα, radiation wavelength 0.71073 Å, final R indices R1 = 0.0984 and wR2 = 0.2645, and R indices (all data) R1 = 0.1434 and wR2 = 0.2987.
(21) (a) Matis, M.; Rapta, P.; Lukeš, V.; Hartmann, H.; Dunsch, L. *J. Phys. Chem. B* **2010**, *114*, 4451. (b) Reynolds, R.; Line, L. L.; Nelson, R. F. *J. Am. Chem. Soc.* **1974**, *96*, 1087.
(22) Connelly, N. G.; Geiger, W. E. *Chem. Rev.* **1996**, *96*, 877.
(23) (a) Sreenath, K.; Thomas, T. G.; Gopidas, K. R. *Org. Lett.* **2011**, *13*, 1134. (b) Murata, H.; Takahashi, M.; Namba, K.; Takahashi, N.; Nishide, H. *J. Org. Chem.* **2004**, *69*, 631.
(24) (a) Hush, N. S. *Prog. Inorg. Chem.* **1967**, *8*, 391. (b) Hush, N. S. *Electrochim. Acta* **1968**, 1005. (c) Hush, N. S. *Coord. Chem. Rev.* **1985**, *64*, 135.
(25) (a) Lancaster, K.; Odom, S. A.; Jones, S. C.; Thayumanavan, S.; Marder, S. R.; Brédas, J.-L.; Coropceanu, V.; Barlow, S. *J. Am. Chem. Soc.* **2009**, *131*, 1717. (b) Heckmann, A.; Amothor, S.; Lambert, C. *Chem. Commun.* **2006**, 2959.
(26) (a) Navale, T. S.; Thakur, K.; Vyas, V. S.; Wadumethrige, S. H.; Shukla, R.; Lindeman, S. V.; Rathore, R. *Langmuir* **2012**, *28*, 71. (b) Lambert, C.; Nöll, G.; Hampel, F. *J. Phys. Chem. A* **2001**, *105*, 7751. (c) Rathore, R.; Burns, C. L.; Abdelwahed, S. A. *Org. Lett.* **2004**, *6*, 1689. (d) Lambert, C.; Nöll, G. *Angew. Chem., Int. Ed.* **1998**, *37*, 2107.
(27) (a) Sui, L.-Z.; Yang, W.-W.; Yao, C.-J.; Xie, H.-Y.; Zhong, Y.-W. *Inorg. Chem.* **2012**, *51*, 1590. (b) Shao, J.-Y.; Yang, W.-W.; Yao, J.; Zhong, Y.-W. *Inorg. Chem.* **2012**, *51*, 4343. (c) Renz, M.; Theilacker, K.; Lambert, C.; Kaupp, M. *J. Am. Chem. Soc.* **2009**, *131*, 16292. (d) Kaupp, M.; Renz, M.; Parthey, M.; Stolte, M.; Würthner, F.; Lambert, C. *Phys. Chem. Chem. Phys.* **2011**, *13*, 16973.
(28) Sheldrick, G. M. *SHELXS97* and *SHELXL97*; University of Göttingen: Göttingen, Germany, 1997.
(29) (a) Becke, A. D. *J. Chem. Phys.* **1993**, *98*, 5648. (b) Lee, C.; Yang, W.; Parr, R. G. *Phys. Rev. B* **1988**, *37*, 785.
(30) Frisch, M. J.; Trucks, G. W.; Schlegel, H. B.; Scuseria, G. E.; Robb, M. A.; Cheeseman, J. R.; Montgomery, J. A., Jr.; Vreven, T.; Kudin, K. N.; Burant, J. C.; Millam, J. M.; Iyengar, S. S.; Tomasi, J.; Barone, V.; Mennucci, B.; Cossi, M.; Scalmani, G.; Rega, N.; Petersson, G. A.; Nakatsuji, H.; Hada, M.; Ehara, M.; Toyota, K.; Fukuda, R.; Hasegawa, J.; Ishida, M.; Nakajima, T.; Honda, Y.; Kitao, O.; Nakai, H.; Klene, M.; Li, X.; Knox, J. E.; Hratchian, H. P.; Cross, J. B.; Adamo, C.; Jaramillo, J.; Gomperts, R.; Stratmann, R. E.; Yazyev, O.; Austin, A. J.; Cammi, R.; Pomelli, C.; Ochterski, J. W.; Ayala, P. Y.; Morokuma, K.; Voth, G. A.; Salvador, P.; Dannenberg, J. J.; Zakrzewski, V. G.; Dapprich, S.; Daniels, A. D.; Strain, M. C.; Farkas, O.; Malick, D. K.; Rabuck, A. D.; Raghavachari, K.; Foresman, J. B.; Ortiz, J. V.; Cui, Q.; Baboul, A. G.; Clifford, S.; Cioslowski, J.; Stefanov, B. B.; Liu, G.; Liashenko, A.; Piskorz, P.; Komaromi, I.; Martin, R. L.; Fox, D. J.; Keith, T.; Al-Laham, M. A.; Peng, C. Y.; Nanayakkara, A.; Challacombe, M.; Gill, P. M. W.; Johnson, B.; Chen, W.; Wong, M. W.; Gonzalez, C.; Pople, J. A. *Gaussian 03*, revision E.01; Gaussian Inc.: Pittsburgh, PA, 2007.

(31) (a) Dunning, T. H.; Hay, P. J. In *Modern Theoretical Chemistry*; Schaefer, H. F., Ed.; Plenum: New York, 1976; Vol. 3, p 1. (b) Hay, P. J.; Wadt, W. R. *J. Chem. Phys.* **1985**, *82*, 270. (c) Wadt, W. R.; Hay, P. J. *J. Chem. Phys.* **1985**, *82*, 284. (d) Hay, P. J.; Wadt, W. R. *J. Chem. Phys.* **1985**, *82*, 299.
(32) (a) Klamt, A.; Schüürmann, G. *J. Chem. Soc., Perkin Trans. 2* **1993**, 799. (b) Andzelm, J.; Kölmel, C.; Klamt, A. *J. Chem. Phys.* **1995**, *103*, 9312. (c) Barone, V.; Cossi, M. *J. Phys. Chem. A* **1998**, *102*, 1995. (d) Cossi, M.; Rega, N.; Scalmani, G.; Barone, V. *J. Comput. Chem.* **2003**, *24*, 669.